Journal of Magnetic Resonance **157,** 210–217 (2002)
doi:10.1006/jmre.2002.2589

Selective Dephasing of OH and NH Proton Magnetization Based on ^{1}H Chemical-Shift Anisotropy Recoupling

K. Schmidt-Rohr[1] and J.-D. Mao

Department of Chemistry, Iowa State University, Ames, Iowa 50011

Received January 18, 2002; revised June 17, 2002; published online August 28, 2002

A method for selectively suppressing the signals of OH and NH protons in ^{1}H combined rotation and multiple-pulse spectroscopy (CRAMPS) and in ^{1}H–^{13}C heteronuclear correlation (HETCOR) solid-state NMR spectra is presented. It permits distinction of overlapping CH and OH/NH proton signals, based on the selective dephasing of the magnetization of OH and NH protons by their relatively large ^{1}H chemical-shift anisotropies. For NH protons, the ^{14}N–^{1}H dipolar coupling also contributes significantly to this dephasing. The dephasing is achieved by a new combination of heteronuclear recoupling of these anisotropies with ^{1}H homonuclear dipolar decoupling. Since the 180° pulses traditionally used for heteronuclear dipolar and chemical-shift anisotropy recoupling would result in undesirable homonuclear dephasing of proton magnetization, instead the necessary inversion of the chemical-shift Hamiltonian every half rotation period is achieved by inverting the phases of all the pulses in the HW8 multiple-pulse sequence. In the HETCOR experiments, carefully timed ^{13}C 180° pulses remove the strong dipolar coupling to the nearby ^{13}C spin. The suppression of NH and OH peaks is demonstrated on crystalline model compounds. The technique in combination with HETCOR NMR is applied to identify the CONH and NH–CH groups in chitin and to distinguish NH and aromatic proton peaks in a peat humin.

INTRODUCTION

Two-dimensional ^{1}H–^{13}C heteronuclear (HETCOR) nuclear magnetic resonance (NMR) spectroscopy of solids (*1–3*) has proven useful for identifying structural units in complex organic materials such as coals (*4*) and humic substances (*5*). With magnetization filters such as the MELODI sequence, which dephases the often trivial signals of directly carbon-bonded protons (*6*), the HETCOR spectra can be simplified and their information content further enhanced.

In this paper, we present a new filter approach, based on dephasing of ^{1}H magnetization of OH and NH protons by the ^{1}H chemical shift anisotropy (CSA) and the ^{14}N–^{1}H dipolar couplings. Thus, overlapping aromatic CH and amide NH or OH and OCH proton signals can be separated. This is particularly useful in natural organic matter, where peak overlap is severe.

While the CSA parameter $|\delta|$ is less than 5 ppm for most protons in C–H bonds, OH protons have larger CSAs of $|\delta| =$ 15–20 ppm (*7*). NH protons have CSAs of $|\delta| = 10$ ppm (*7, 8*) and are also subject to dephasing by the ^{14}N–^{1}H dipolar coupling, which affects 2/3 of their magnetization with a coupling of $2 * |\delta_{\mathrm{NHd}}| = 2 * 8$ kHz. As shown in Fig. 1, after only a short CSA dephasing time, the signals of OH groups are strongly suppressed, while the C–H signals are only slightly reduced in intensity. At the same dephasing time, the N–H proton signal is also more than fivefold reduced in intensity, compared to the aromatic C–H signal.

We achieve the dephasing by recoupling of the ^{1}H CSA and ^{14}N–^{1}H dipolar coupling, while decoupling the ^{1}H homonuclear dipolar interaction by a multiple-pulse sequence. Trains of rotation-synchronized 180° pulses as used for ^{13}C CSA recoupling (*9–11*) would lead to undesirable homonuclear dephasing during the 180° pulses. Instead, we use a scheme of inverting the average chemical-shift and ^{14}N–^{1}H dipolar Hamiltonians every half rotation period. This filter proves useful not only in HETCOR NMR, but also with direct ^{1}H detection, i.e., combined rotation and multiple-pulse spectroscopy (CRAMPS) (*12*), where it facilitates peak assignment. When the ^{1}H CSA filter is applied before HETCOR NMR, care must be taken to decouple the ^{13}C–^{1}H dipolar interaction by ^{13}C 180° pulses. The new method is demonstrated on OH- and NH-containing model compounds and on natural organic matter.

THEORETICAL BACKGROUND

Anisotropic Couplings of OH and NH

Multiple-pulse NMR studies (*13*) have shown that C–H protons, whether bonded to aliphatic or aromatic moieties, have chemical-shift anisotropy widths $\Delta\sigma = |\sigma_{11} - \sigma_{33}|$ of only $\Delta\sigma \leq 8$ ppm, and correspondingly chemical-shift anisotropy parameters $|\delta| = \max(|\sigma_{\mathrm{nn}} - \sigma_{\mathrm{iso}}|)$ of $|\delta| \leq 5$ ppm, or 2 kHz at 400 Hz/ppm (*7, 13*). The chemical-shift anisotropies of N–H and O–H protons that have been reported in the literature are significantly larger. The widely studied COOH protons have

[1] To whom correspondence should be addressed. Fax: 515-294-0105. E-mail: srohr@iastate.edu.

1090-7807/02 $35.00

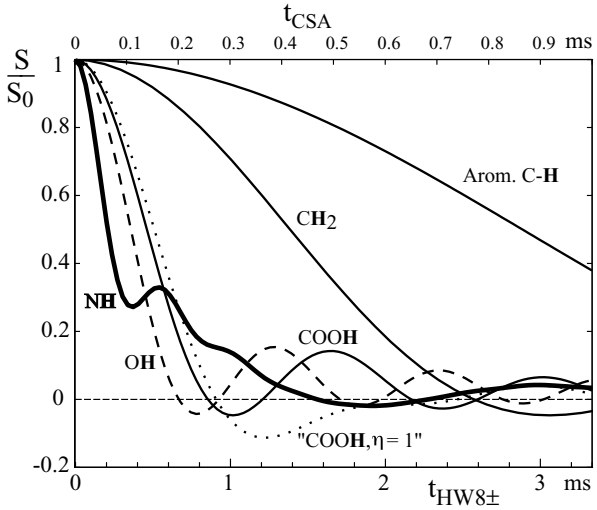

FIG. 1. Simulated dephasing curves under REDOR-like ^{1}H CSA recoupling, based on literature data (*7*). The principal values used were (11.7, 8.2, 5.1) ppm for aromatic H; (5.6, 4.8, −1.7) ppm for methylene protons; (22, 20, 0) ppm for COOH (full line); (22, 11, 0) ppm for "COOH $\eta = 1$" (dotted line); (14, 14, −13) for OH (dashed line); and (14.4, 12.5, −21) for NH (thick line), at 400 Hz/ppm. Two-thirds of the NH proton magnetization also dephase under the (−8, −8, 16) kHz ^{14}N–^{1}H dipolar coupling. The regular CSA-dephasing time is given at the top, while the time axis at the bottom takes into account the theoretical scaling factor of 0.33 of the HW8 homonuclear decoupling sequence (see Fig. 2).

$\Delta\sigma = 18 - 24$ ppm ($|\delta| = 15$ ppm or 6 kHz at 400 Hz/ppm) (*7, 13*). The few hydroxyl O–H protons that have been investigated (*7*) have similar, if not larger, $\Delta\sigma$ values of ca. 30 ppm ($|\delta| = 20$ ppm). Amide protons have $\Delta\sigma \sim 16$ ppm, corresponding to $|\delta| = 10$ ppm, or 4 kHz at 400 Hz/ppm (*7, 8, 14*).

In addition to the CSA dephasing, N–H protons also experience the ^{14}N–^{1}H dipolar coupling of $|\delta_{NH}| = 8$ kHz. Since ^{14}N is a spin-1 nucleus, two-thirds of the amide proton magnetization, corresponding to the two outer of the three "transitions" or to the $m = \pm 1$ ^{14}N quantum states, dephase very quickly under the influence of the doubled ^{14}N–^{1}H dipolar coupling ($2 * \delta_{NH} = 16$ kHz). One third, corresponding to the central or $m = 0$ "transition", remains unaffected (in the high-field approximation). In the following, for brevity we will refer to the recoupling sequence as CSA recoupling or CSA filtering, but it should be kept in mind that it also reintroduces the ^{1}H heteronuclear couplings, in particular the ^{14}N–^{1}H interaction which helps with the amide-proton dephasing.

Principle of the CSA Filter

The block diagram of the CSA-filter pulse sequence is presented in Fig. 2. It consists of the OH and NH dephasing filter, typically of duration $2\,t_r$, followed by a regular CRAMPS (a) or HETCOR (c) experiment.

The filter requires homonuclear decoupling of the protons and evolution under the CSA while the isotropic chemical shift is refocused. Under magic-angle spinning (MAS), the CSA must be recoupled by a suitable pulse sequence. Two 180° pulses per rotation period t_r, spaced by $t_r/2$ as in standard REDOR, will recouple the CSA and ^{14}N–^{1}H interactions (*11, 15*).

However, a simple REDOR-like approach will work only at very high spinning frequencies, where MAS achieves homonuclear decoupling (*16*). At the standard spinning frequencies of ca. 5 kHz used widely for samples of low sensitivity, pulsed homonuclear decoupling (*17*) is necessary. Under such a pulse sequence, the intensity after N rotation periods t_r of CSA recoupling will be (*15*)

$$S(Nt_r)/S_0 = \langle \cos\{2\pi\, 2Nt_r c_{sf}\,(S_1 \cos\gamma - C_1 \sin\gamma)\}\rangle. \quad [1]$$

Here, C_1 and S_1 are coefficients that depend on the chemical-shift principal values and the polar coordinates (α, β) of the rotor axis in the CSA principal-axes system, as listed in Ref. (*18*). For uniaxial interactions ($\eta = 0$), such as heteronuclear dipolar couplings in REDOR, the S_1 term vanishes, but for the CSAs of interest here, this is not generally the case. The pointed brackets indicate the powder average, which removes the dependence on the tensor orientation, including the rotation angle γ around the rotor axis. The scaling factor c_{sf} takes into account the reduction of the CSA and heteronuclear dipolar coupling by the multiple-pulse decoupling sequence (*13*). The factor of 2π

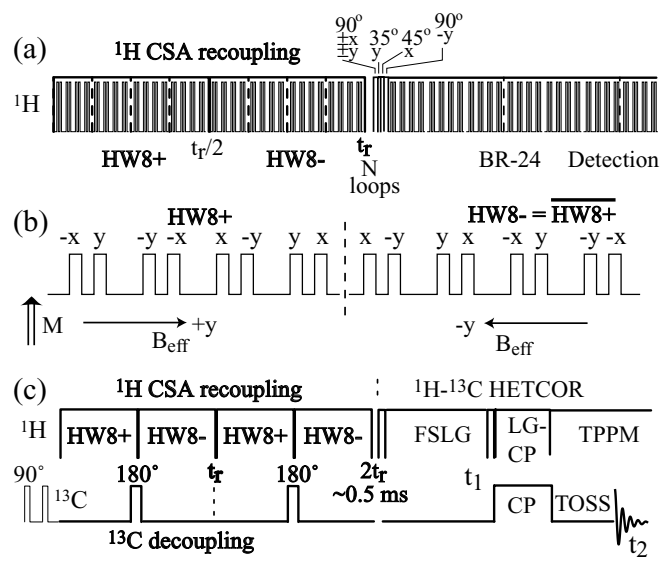

FIG. 2. Pulse sequences for dephasing of ^{1}H signals with large chemical-shift anisotropies. (a) ^{1}H CSA dephasing followed by CRAMPS detection. The alternation of HW8+ and HW8− pulse sequences achieves recoupling of the ^{1}H CSA without the use of 180° pulses. (b) Pulse diagram of the HW8+ and HW8− sequences. (c) Block diagram of the ^{1}H CSA dephasing followed by 2D HETCOR NMR, with frequency-switched Lee–Goldburg (FSLG) irradiation for homonuclear decoupling during ^{1}H evolution and Lee–Goldburg cross polarization (LG-CP), which prevents spin diffusion. Total suppression of sidebands (TOSS) was applied before detection under heteronuclear decoupling by two-pulse phase modulation (TPPM). The ^{13}C 180° pulses during the ^{1}H CSA filtering prevent recoupling of the ^{13}C–^{1}H dipolar coupling. The initial 90° pulses on ^{13}C destroy any direct ^{13}C magnetization that might be present.

appears in Eq. [1] because in this paper, the anisotropy parameter δ does not contain this factor.

The dephasing curves of Fig. 1 were calculated based on Eq. [1]. As in REDOR, the decay under the recoupled anisotropic interaction exhibits only relatively weak oscillations for an unoriented sample. Therefore, the signals of sites with large CSAs die down quickly, leading to quite clean OH and NH suppression after just a relatively short filter time period.

CSA and Heteronuclear Recoupling of ^{1}H without 180° Pulses

The standard recoupling of heteronuclear dipolar interactions or of chemical-shift anisotropies with two 180° pulses per rotation period is less than optimum in the present case. During the 180° pulses, homonuclear dipolar dephasing of proton magnetization will occur because the homonuclear dipolar coupling is not averaged to zero. Given that the duration of the two 180° pulses per rotation period adds up to 16 μs, this dephasing reduces the ^{1}H magnetization significantly.

According to one valid viewpoint, it is the purpose of the 180° pulses in REDOR *(15)* or CODEX (*11*) experiments to invert the sign of the anisotropic frequency every half rotation period. Thus, if we invert the sign of the CSA Hamiltonian every $t_r/2$, we will achieve the same recoupling result. By means of the multiple-pulse homonuclear decoupling sequence, the average Hamiltonian can indeed be manipulated in this fashion.

With the widely used MREV8 sequence, inversion of the z-component of the average chemical-shift Hamiltonian is not easily possible. Therefore, we have instead chosen the Haeberlen–Waugh 8-pulse (HW8) (*19, 20*) sequence (see Fig. 2b), which has a purely transverse effective field, along the y-axis. HW8 has been shown to be a well-compensated, robust homonuclear decoupling sequence similar in performance to MREV8 (*19, 20*). The only potential drawback is the relatively small scaling factor of $c_{sf} = 0.33$ of HW8, which is 30% smaller than that of MREV8.

For HW8, inversion of all pulses inverts the average chemical-shift Hamiltonian, e.g., from $+y$ to $-y$. We will refer to the original and inverted sequence as HW8+ and HW8−, respectively; see Fig. 2b. The original and the inverted sequence are both well-compensated HW8 sequences, and therefore the homonuclear decoupling performance is good.

Since the effective field of HW8 is completely transverse, no initial excitation pulse is needed. The magnetization remaining after the filter is along the z-axis. Thus, the regular CRAMPS or HETCOR sequence can follow without modification.

In order to obtain the normalized CSA dephasing $S(Nt_r)/S_0$, a sequence for measuring the reference signal S_0 without CSA dephasing but with the same T_2 decay is desirable. It can be generated by simply swapping HW8+ and HW8− in every other rotation period, resulting in a sequence HW8+ $(t_r/2)$ HW8− (t_r) HW8− $(3t_r/2)$ HW8+ $(2t_r)$ within a pair of rotation periods. This sequence is also very useful for testing and optimizing the performance of the HW8± sequences. It refocuses all interactions in an echo, whose height can be maximized by varying the pulse length. Overall, since the optimum filter times for OH and NH suppression are relatively short (ca. 8 HW± cycles), the ^{1}H CSA filter is relatively insensitive to pulse imperfections.

CRAMPS Detection

Multiple-pulse decoupling works best at lower spinning frequencies (1–3 kHz), since the multiple-pulse sequences were designed assuming quasi-static dipolar couplings (*12, 17*). Thus, with CRAMPS ^{1}H detection as indicated in Fig. 2a, lower spinning speeds should be used than for ^{13}C detection in the HETCOR version. Note, however, that at very low spinning frequencies, the OH and NH proton signals will lose intensity to sidebands, which arise due to the large CSA and ^{14}N–^{1}H interactions. In order to avoid significant sidebands, the spinning frequency should exceed the multiple-pulse-scaled anisotropy δ, e.g., 15 ppm $*$ 0.48 = 7 ppm, which is 2.8 kHz at 400 Hz/ppm, because this places the sidebands outside the static powder pattern. The CRAMP spectra shown below were taken at 2.083 kHz, so the sidebands may be detectable.

^{1}H CSA Filtering in HETCOR Experiments

As outlined in the Introduction, useful structural information on many organic solids can be obtained by combining the ^{1}H chemical-shift information with ^{13}C detection, in a 2D HETCOR experiment. By applying the CSA filter before a HETCOR experiment, we can identify cross peaks of OH and NH protons with specific carbons. The filtered spectrum is a correlation of ^{13}C signals with those of C–H protons exclusively (except for potential contributions from rotating NH_3 groups). The HETCOR experiments (*6*) used frequency-switched Lee–Goldburg (FSLG) (*21*) irradiation for homonuclear decoupling during ^{1}H evolution. Lee–Goldburg cross polarization (LG-CP), which prevents spin diffusion, and total suppression of sidebands (TOSS) by four 180° pulses (*22*) were applied before detection under heteronuclear decoupling by two-pulse phase modulation (TPPM) (*23*).

For the implementation of the ^{1}H CSA filter before the HETCOR experiment, it is crucial to realize that many of the protons detected in HETCOR spectra are subject to ^{13}C heteronuclear dipolar couplings that are comparable to, or even exceed, the ^{1}H CSA and ^{14}N–^{1}H dipolar coupling exploited for dephasing. Even though the average proton has a dipolar coupling of less than 100 Hz to ^{13}C, the HETCOR experiment selects precisely those protons that are close to the detected ^{13}C nuclei, with C–H couplings of several kHz (*6*). The ^{13}C–^{1}H dipolar coupling can be removed by suitably timed 180° pulses on the ^{13}C channel. While in principle a single ^{13}C pulse in the middle of the filter period suffices, in practice one ^{13}C pulse in the middle of each rotation period was found to work well. Due to the large size (~20 kHz) of the one-bond C–H dipolar coupling, the timing of the ^{13}C pulses must be controlled precisely. Even

a few microseconds of C–H dephasing lead to significant reductions of the signals of protonated carbons. Nevertheless, once the timings have been programmed accurately, this issue does not need to be considered further.

In order to obtain strong signals of aromatic carbons, the spinning speed must be sufficiently high. Since very fast spinning degrades the homonuclear decoupling performance of the HW8 sequence, a spinning frequency near 5 kHz is reasonable as a compromise. We used four cycles of HW8 per rotation period in the ^{1}H CSA-filtered HETCOR experiments. Longer times may lead to more perfect OH and NH suppression, but also decrease CH signals by their own CSA dephasing and by T_2 relaxation. Note that with a signal-to-noise ratio of X, an X-fold signal suppression is completely sufficient.

RESULTS AND DISCUSSION

We demonstrate the new experiments first on three NH- and OH-containing model compounds and then show its applicability for identifying structural units in natural organic matter and complex organic molecules.

CSA Dephasing with CRAMPS Detection

Figure 3a shows the effect of the ^{1}H CSA dephasing on the peaks in the CRAMP spectrum of fumaric acid monoethyl ether.

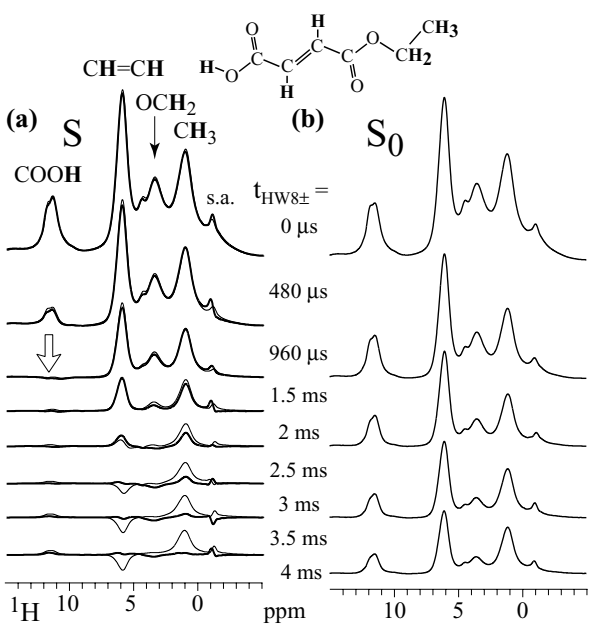

FIG. 3. Series of CRAMP ^{1}H spectra of fumaric acid monoethyl ester at 2.083 kHz with increasing HW8± ^{1}H CSA dephasing times Nt_r, as indicated (above 1 ms, rounded to the nearest 0.5 ms). Recycle delay: 3 s, 128 scans per spectrum. (a) Spectra with irradiation near 4 ppm (thin line) and near 0 ppm (thick line) during the ^{1}H CSA filter. The arrow marks the complete suppression of the OH proton signal after 960 μs of HW8± CSA dephasing. Label "s.a.": spinning artifact. (b) Corresponding reference spectra with swapped sequence HW8+ (t_r/2) HW8− (t_r) HW8− (3t_r/2) HW8+ (2t_r) that cancels ^{1}H CSA dephasing. Here, the "dephasing" period must be an even multiple of the rotation period.

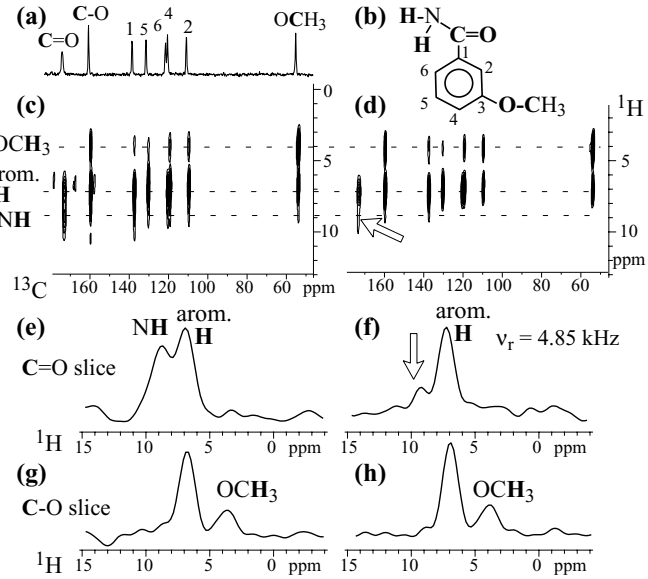

FIG. 4. Dephasing of the NH proton signal in the HETCOR spectrum of 3-methoxy benzamide, at $\nu_r = 4845$ Hz, 6-s recycle delay. (a) CP/MAS/TOSS ^{13}C spectrum, with frequency axis matched to the HETCOR spectrum in (c). (b) Structure of the molecule. (c) Full reference 2D HETCOR spectrum, with 64 t_1 increments. (d) Corresponding HETCOR spectrum after two rotation periods of ^{1}H CSA and ^{14}N–^{1}H dipolar recoupling, 32 scans per t_1 increment. (e, f) Cross sections through the C=O resonance position of the spectra in (c) and (d), respectively, demonstrating the suppression of the NH proton resonance. (g, h) Cross sections at the aromatic C–O resonance position, which show peaks of aromatic and OCH_3 protons, for the spectra in (c) and (d), respectively.

The preferential dephasing of the COOH protons within two rotation periods of CSA recoupling by HW8± is clearly observed. Two series of spectra, taken with a 4-ppm difference in irradiation frequency during the CSA filter, are shown superimposed. The good agreement at short and intermediate dephasing times confirms the reliability of the pulse sequence, and also shows that effects of differential isotropic chemical-shift evolution are not responsible for the selective dephasing. Corresponding reference spectra (S_0) with the same T_2 relaxation delays but no CSA dephasing under HW8+ (t_r/2) HW8− (t_r) HW8− (3t_r/2) HW8+ (2t_r) irradiation are shown in Fig. 3b.

NH Dephasing in HETCOR Spectra

In Fig. 4, amide-proton signal suppression by the OH/NH dephasing sequence is demonstrated on 3-methoxy-benzamide, using ^{13}C detection in a HETCOR experiment. First, the peaks in the ^{13}C CP/TOSS spectrum (Fig. 4a) can be assigned based both on their chemical shifts and on the cross peaks to OCH_3 protons in the regular HETCOR spectrum, Fig. 4c. The cross section of the C=O resonance shows two peaks near 7 and 9 ppm. The tentative assignment of the 9-ppm band to the NH protons is clearly confirmed by the dephasing of this peak during a 2t_r (413-μs) ^{1}H CSA dephasing period with HW8± recoupling, Fig. 4d. For clarity, cross sections at the C=O resonance are shown in Figs. 4e and 4f. Other slices, for instance at the C–O

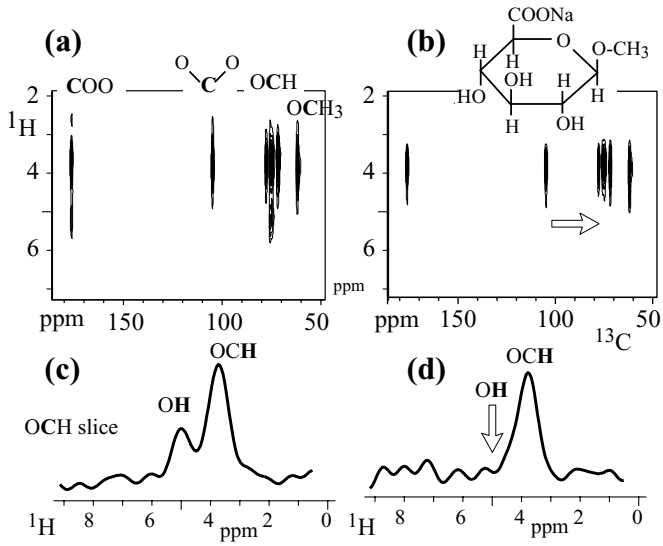

FIG. 5. Dephasing of the OH proton signal in the HETCOR spectrum of methyl β-D-glucuronide (structure shown in inset) at $\nu_r = 4845$ Hz, with 14-s recycle delay and 80 t_1 increments. (a) Regular HETCOR spectrum for reference, 16 scans per t_1 increment. (b) HETCOR spectrum after two rotation periods of ^{1}H CSA (and ^{14}N–^{1}H dipolar) recoupling, 32 scans per t_1 increment. (c, d) Cross sections through the 75-ppm OCH resonance of the spectra in (a) and (b), respectively, demonstrating the suppression of the NH proton resonance.

resonance as shown in Figs. 4f, 4g, are not affected by the CSA filter.

OH Dephasing in HETCOR Spectra

In Fig. 5, the application of the new filtered-HETCOR method to a carbohydrate (methyl β-D-glucuronide) is demonstrated. In addition to the dominant OCH proton signal, several ^{13}C signals, for instance at 75 and 177 ppm, in the HETCOR spectrum, Fig. 5a, have cross peaks with protons at a slightly more downfield chemical shift. This upfield ^{1}H component is also seen as a clear peak in the cross section of Fig. 5c. Its tentative assignment to OH protons is confirmed by the ^{1}H CSA dephasing. Figures 5b, 5d show that HW8± filtering of 0.5-ms duration suppresses this signal to the noise level.

Application to Chitin

In order to demonstrate the usefulness of the OH and NH suppression experiment for peak assignment in complex organic solids, we show the identification of the CO–NH group in chitin. Chitin is an insoluble polysaccharide with *N*-acetyl (CH_3–CO–NH) sidegroups, see the structure in Fig. 6. It makes up the exoskeleta of insects and other arthropods. Various organisms produce other partially *N*-acetylated polysaccharides.

Figure 6a shows the TOSS spectrum of chitin. Figures 6c and 6d compare the regular HETCOR spectrum of chitin, taken at $\nu_r = 4845$ Hz, with the HETCOR spectrum after NH and OH suppression. The NH cross peaks near 8 ppm are suppressed in the 2D spectrum. This is confirmed in the cross sections at the CO resonance, Figs. 6e, 6f.

Application to Peat Humin

In humic substances, COO groups play a major role in nutrient release and heavy metal binding. Previously, the typical peak near 173 ppm has often been characterized as carboxylic acid groups (*24*). On the other hand, the relatively large nitrogen content (typically, C : N = 10 : 1) suggests a significant fraction of CO–NH groups (*25, 26*). With the present experiment, we can identify these moieties. The results for a peat humin are shown in Fig. 7. The pronounced shoulder around 7–9 ppm in the COO/CON cross section is almost completely suppressed by 0.5 ms of HW8± CSA dephasing. This shows that this signal is dominated by NH protons, while aromatic protons hardly contribute. The spectrum after dephasing thus allows us to obtain a more correct estimate of the fraction of COO groups bonded to aromatic rings. Note that the 2D spectrum confirms that the dephasing is not due to isotropic-shift differences: the signals of aromatic proton bonded to aromatic carbons are not dephased.

Application to 1,8-Dihydroxy-3-methylanthraquinone

Another example of structural information obtained from ^{1}H CSA dephasing is shown in the application to 1,8-dihydroxy-3-methylanthraquinone; see Figs. 8 and 9. The HETCOR spectrum, Fig. 8, helps to assign the ^{13}C resonances to most sites in the molecule. However, the assignment of the proton peak

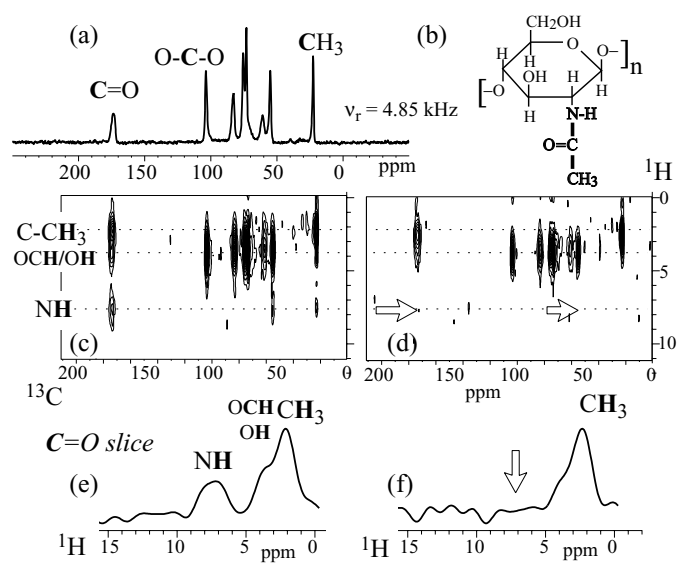

FIG. 6. Spectra of chitin at $\nu_r = 4845$ Hz. (a) CP/MAS/TOSS ^{13}C spectrum. (b) Simplified structure of the repeat unit of chitin, with *N*-acetyl group highlighted. (c) Regular HETCOR spectrum, with 1.3-s recycle delay and 64 t_1 increments, 128 scans per t_1 increment. (d) HETCOR spectrum after two rotation periods of ^{1}H CSA (and ^{14}N–^{1}H dipolar) recoupling; the number of scans per t_1 increment was 384. (e, f) Cross sections at the C=O resonance of the spectra in (c) and (d), respectively.

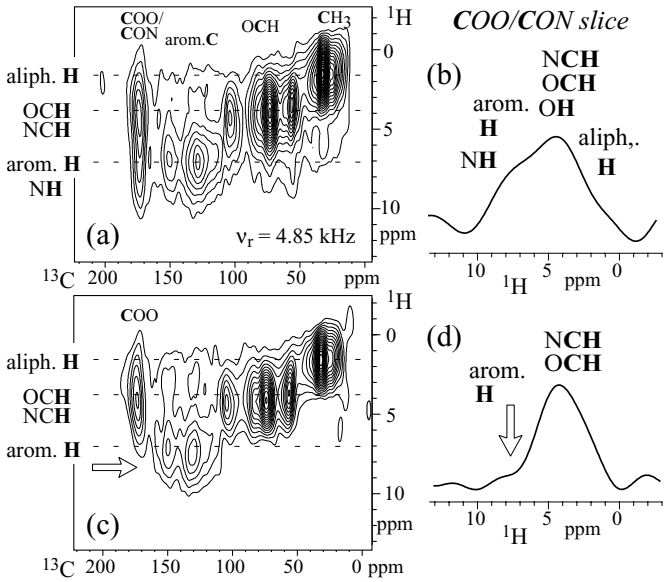

FIG. 7. HETCOR spectra of a peat humin at $\nu_r = 4845$ Hz, with 40 t_1 increments and 0.36-s recycle delay. (a) Regular reference spectrum, and (b) cross section at 172 ppm, with 800 scans per t_1 increment. (c) Spectrum after two rotation periods of ^{1}H CSA (and ^{14}N–^{1}H dipolar) recoupling, and (d) cross section at 172 ppm, with 4096 scans per t_1 increment.

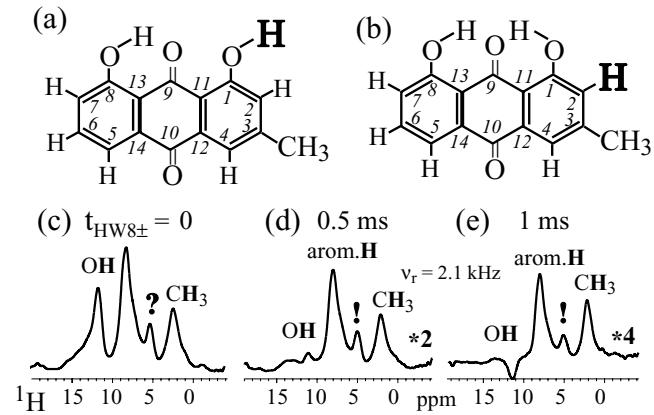

FIG. 9. (a, b) Two hypothetical structures of 1,8-dihydroxy-3-methylanthraquinone, with the putative 5.5-ppm proton highlighted. (c–e) Series of ^{1}H CSA dephased CRAMP spectra after (c) 0, (d) 480 μs, (e) 960 μs of dephasing, at $\nu_r = 2.083$ kHz, with 4, 16, and 32 scans, respectively, using 60-s recycle delays. The lack of dephasing of the 5.5-ppm peak (marked by ? and !) indicates that it is the signal of an aromatic proton, in agreement with structure (b).

at 5.5 ppm (marked by an arrow) is not immediately obvious. Given the aromatic and OH protons in the structure, a signal near 5.5 ppm might traditionally be assigned to OH protons. This would suggest the structure of Fig. 9a, where the OH proton in bold would be assigned to the 5.5-ppm peak. However, this is refuted by the ^{1}H CSA dephasing data of Figs. 9c–9e. While the hydrogen-bonding protons near 12 ppm dephase completely within less than 1 ms, the peak at 5.5 ppm dephases only as slowly as the main aromatic peak near 8 ppm. This strongly suggests that the proton resonating at 5.5 ppm is itself an aromatic proton, as predicted by the structure of Fig. 9b. Aromatic-proton resonances shifted by several ppm from the standard aromatic shift range have indeed been observed in a number of highly aromatic solids, and explained in terms of ring-current effects associated with π-electrons in aromatic moieties (*27*).

This result is fully consistent with all the other NMR data. For instance, the intensities in the CRAMP spectrum confirm that both OH protons resonance near 12 ppm. Similarly, the cross section through the HETCOR spectrum at 150 ppm shows that carbon 3 is separated by the same distance from the proton at 5.5 ppm and from one aromatic proton, as in the structure of Fig. 9b, while in the structure of 9a carbon 3 is nearer to two aromatic protons than to the putative 5.5 ppm OH proton.

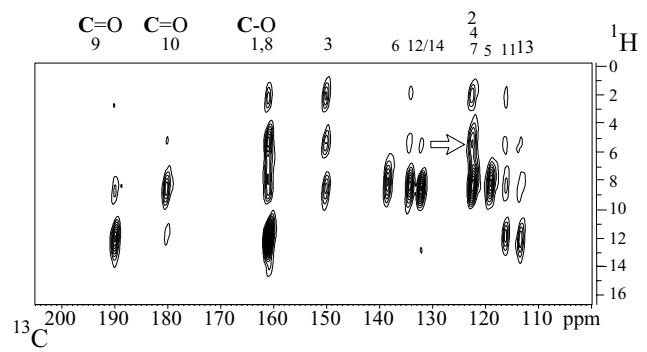

FIG. 8. Regular HETCOR spectrum of 1,8-dihydroxy-3-methylanthraquinone (see structure in Fig. 9 below), recorded at $\nu_r = 5053$ Hz, with 64 t_1 increments, 60-s recycle delay, and 16 scans per t_1 increment. The numbering of carbon peaks at the top matches the structures shown in Fig. 9. The unexpected ^{1}H peak near 5.5 ppm is marked by an arrow.

Assessment

The technique presented here is particularly valuable for identification of OH protons, and of NH protons in HETCOR spectra. In CRAMPS applications, NH proton selection can be achieved more cleanly by ^{14}N–^{1}H double resonance, using, for instance, a ^{14}N–^{1}H version of the recently introduced SPIDER technique (*28*) combined with the HW8± recoupling scheme introduced here. Nevertheless, the present technique is technically simpler, requiring no ^{14}N irradiation, and achieves NH suppression more efficiently. This is valuable for isolating aromatic-proton signals. It is readily combined with HETCOR spectroscopy, which already requires multiple-pulse decoupling.

The CRAMPS-detected version of the new experiment provides an example of ^{1}H filter techniques that will make CRAMPS NMR studies more structurally informative. Even with the relatively poorly resolved CRAMPS acquired in a 7-mm double-resonance probehead for this paper, useful structural information has been obtained (see Fig. 9). In a dedicated

CRAMPS probehead, higher resolution can be achieved and more detailed studies will be possible, including combinations of the CSA filter with two-dimensional exchange spectroscopy (*29*). Potentially, the selective CSA-based suppression of the magnetization of certain types of protons can also be used in ^{1}H spin-diffusion studies (*30*). With the high sensitivity of CRAMPS detection, the technique presented here makes it conveniently possible to obtain good estimates of the chemical-shift anisotropy of many proton sites. By identifying the structural information contained in these data, it also provides an incentive for such ^{1}H CSA studies.

CONCLUSIONS

We have introduced a technique for selectively suppressing OH and NH proton peaks relative to CH proton signals, based on ^{1}H CSA dephasing. It is achieved quite efficiently by a new approach that combines CSA recoupling with multiple-pulse homonuclear decoupling by inversion of the CSA average Hamiltonian while retaining good homonuclear decoupling. In particular, this avoids homonuclear dipolar dephasing during 180° recoupling pulses. The method works not only on crystalline model compounds, but is efficient enough to be applicable to complex natural organic matter. It increases the structural information of ^{1}H CRAMP and ^{1}H–X-nucleus HETCOR spectra significantly.

EXPERIMENTAL

Samples

Several model compounds were purchased from Sigma–Aldrich–Fluka for these experiments: fumaric acid monoethyl ester, 3-methoxy benzamide, methyl β-D-glucuronide, 1,8-dihydroxy-3-methylanthraquinone, and chitin (poly(N-acetyl-1,4-β-D-glucopyranosamine)) from crab shells. In order to demonstrate the applicability of this technique to complex natural organic matter, a peat humin (the insoluble organic fraction of peat) was also used in this study. This humin was extracted from Florida Pahokee peat provided by the International Humic Substances Society (IHSS). The extraction procedures have been described in detail elsewhere (*24*).

NMR Parameters

Experiments were performed in a Bruker DSX400 spectrometer at 400 MHz for ^{1}H and 100 MHz for ^{13}C, using a 7-mm magic-angle spinning probehead. No special tune-up of the spectrometer, other than optimization of the pulse lengths, was performed for the experiments. The ^{1}H 90°-pulse length was 3.7 μs, the slightly longer (*13, 20*) optimum pulse length in the BR24 detection 4 μs. The sum of the pulse length plus short window of the BR24 used for detection was 5.5 μs, corresponding to a long window of 7 μs. The spinning speeds was 2.083 kHz for CRAMPS detection with BR24 multiple-pulse decoupling (*31*). Slow spinning is known to provide the best CRAMPS resolution. The rotation period accommodates 8 cycles of HW8, each with a cycle time of $12 * 5$ μs.

In the HETCOR experiments, at $\nu_r = 4845$ Hz, four cycles of the HW8($\pm$) sequence (*19, 20*), with $12 * 4.3$ μs cycle time and 3.8-μs pulses, were applied per rotation period of ^{1}H CSA filtering. Frequency-switched Lee–Goldburg (*32*) homonuclear ^{1}H decoupling with a 60-kHz effective field strength and a 66-μs dwell time was used during evolution. The number of t_1 increments was between 40 and 80. Cross-polarization with a magic-angle spinlock of the proton magnetization was applied for 0.5 ms. Four-pulse total suppression of sidebands (TOSS) (*22*) was used. During ^{13}C detection, the ^{1}H decoupling power was $\gamma B_{1,H}/2\pi = 64$ kHz and TPPM decoupling was applied. Spectra were run overnight, i.e., with 256–1024 scans averaged per t_1 increment. The recycle delay and number of scans for each spectrum is given in the corresponding figure caption.

ACKNOWLEDGMENTS

The authors thank Mei Hong for her help with the setup of the HETCOR experiments with FSLG decoupling. Financial support by the Department of Chemistry and College of Agriculture, Iowa State University, is gratefully acknowledged.

REFERENCES

1. P. Caravatti, L. Braunschweiler, and R. R. Ernst, Heteronuclear correlation spectroscopy in rotating solids, *Chem. Phys. Lett.* **100,** 305–310 (1983).
2. B. J. vanRossum, H. Forster, and H. J. M. de Groot, High-field and high-speed CP-MAS ^{13}C NMR heteronuclear dipolar correlation spectroscopy of solids with fequency-switched Lee–Goldberg homonuclear decoupling, *J. Magn. Reson.* **124,** 516–519 (1997).
3. A. Lesage, S. Sakellariou, S. Steuernagel, and L. Emsley, Carbon-proton chemical-shift correlation in solid-state NMR by through-bond multiple-quantum spectroscopy, *J. Am. Chem. Soc.* **120,** 13194–13201 (1998).
4. M. A. Wilson, J. V. Hanna, K. B. Anderson, and R. E. Botto, ^{1}H CRAMPS NMR derived hydrogen distributions in various coal macerals, *Org. Geochem.* **20,** 985–999 (1993).
5. J. D. Mao, B. Xing, and K. Schmidt-Rohr, New structural information on a humic acid from two-dimensional ^{1}H–^{13}C correlation solid-state nuclear magnetic resonance, *Environ. Sci. Technol.* **35,** 1928–1934 (2001).
6. X. L. Yao, K. Schmidt-Rohr, and M. Hong, Medium- and long-distance ^{1}H–^{13}C heteronuclear correlation NMR in solids, *J. Magn. Reson.* **149,** 139–143 (2001).
7. T. M. Duncan, "A Compilation of Chemical Shift Anisotropies." Farragut, Chicago (1997).
8. A. Ramamoorthy, C. H. Wu, and S. J. Opella, Three-dimensional solid-state NMR experiment correlating chemical shift and dipole coupling of two heteronuclei, *J. Magn. Reson.* **107,** 88–90 (1995).
9. R. Tycko, G. Dabbagh, and P. Mirau, Determination of chemical-shift-anisotropy lineshapes in a two-dimensional magic-angle-spinning NMR experiment, *J. Magn. Reson.* **85,** 265–274 (1989).
10. M. Hong, Solid-state NMR determination of ^{13}Cα chemical shift anisotropy for the identification of protein secondary structure, submitted for publication.

11. E. R. deAzevedo, W.-G. Hu, T. J. Bonagamba, and K. Schmidt-Rohr, Principles of centerband-only detection of exchange in solid state NMR, and extentions to four-time CODEX, *J. Chem. Phys.* **112,** 8988–9001 (2000).

12. B. C. Gerstein, C. Chow, R. G. Pembleton, and R. C. Wilson, Utility of pulse nuclear magnetic resonance for studying protons in coals, *J. Phys. Chem.* **81,** 565–570 (1977).

13. U. Haeberlen, "High Resolution NMR of Solids," *Adv. Magn. Reson.*, Supplement 1, Academic Press, San Diego (1976).

14. R. Gerald II, T. Bernhard, U. Haeberlen, J. Rendell, and S. Opella, Chemical shift and EFG tensors for the amide and carboxyl 1Hs in the model peptide: Single crystal ^{2}H NMR, *J. Am. Chem. Soc.* **115,** 777–782 (1993).

15. T. Gullion and J. Schaefer, Rotational-echo double-resonance NMR, *J. Magn. Reson.* **81,** 196–200 (1989).

16. R. Graf, D. E. Demco, J. Gottwald, S. Hafner, and H. W. Spiess, Dipolar couplings and internuclear distances by double-quantum NMR spectroscopy of solids, *J. Chem. Phys.* **106,** 885–895 (1997).

17. J. S. Waugh, L. M. Huber, and U. Haeberlen, Approach to high-resolution NMR in solids, *Phys. Rev. Lett.* **20,** 180–182 (1968).

18. K. Schmidt-Rohr and H. W. Spiess, "Multidimensional Solid-State NMR and Polymers," 1st ed., Academic Press, London (1994).

19. U. Haeberlen and J. S. Waugh, Coherent averaging effects in magnetic resonance, *Phys. Rev.* **175,** 453–467 (1968).

20. M. Mehring, "Principles of High-Resolution NMR in Solids," 2nd ed., Springer-Verlag, Heidelberg (1983).

21. A. Bielecki, A. C. Kolbert, H. J. M. de Groot, R. G. Griffin, and M. H. Levitt, Frequency-switched Lee–Goldburg sequences in solids, *Adv. Magn. Reson.* **14,** 111–124 (1990).

22. W. T. Dixon, Spinning-sideband-free and spinning-sideband-only NMR spectra of spinning samples, *J. Chem. Phys.* **77,** 1800–1809 (1982).

23. A. E. Bennett, C. M. Rienstra, M. Auger, K. V. Lakshmi, and R. G. Griffin, Heteronuclear decoupling in rotating solids, *J. Chem. Phys.* **103,** 6951–6958 (1995).

24. F. J. Stevenson, "Humus Chemistry: Genesis, Composition, Reactions," 2nd ed., Wiley, New York (1994).

25. L. Benzing-Purdie, J. A. Ripmeester, and C. M. Preston, Elucidation of the nitrogen form in melanoidins and humic acid bu nitrogen-15 cross polarization magic-angle spinning nuclear magnetic resonance spectroscopy, *J. Agr. Food Chem.* **31,** 913–915 (1983).

26. H. Knicker, R. Fründ, and H.-D. Lüdemann, The chemical nature of nitrogen in native soil organic matter, *Naturwissenschaften* **8,** 219–211 (1993).

27. C. Ochsenfeld, S. P. Brown, I. Schnell, J. Gauss, and H. W. Spiess, Structure assignment in the solid state by the coupling of quantum-chemical calculations with NMR experiments: A columnar hexabenzacoronene derivative, *J. Am. Chem. Soc.* **123,** 2597–2606 (2001).

28. K. Schmidt-Rohr and J.-D. Mao, Selective observation of nitrogen-bonded carbons in solid-state NMR by saturation-pulse induced dipolar exchange with recoupling, *Chem. Phys. Lett.* **359,** 403–411 (2002).

29. P. Caravatti, P. Neuenschwander, and R. R. Ernst, Characterization of heterogeneous polymer blends by two-dimensional proton spin diffusion spectroscopy, *Macromolecules* **18,** 119–122 (1985).

30. J. Clauss, K. Schmidt-Rohr, and H. W. Spiess, Determination of domain sizes in polymers, *Acta Polym.* **44,** 1 (1993).

31. D. P. Burum and W. K. Rhim, Analysis of multiple-pulse NMR in solids, III, *J. Chem. Phys.* **71,** 944–956 (1979).

32. A. Bielecki, A. C. Kolbert, and M. H. Levitt, Frequency-switched pulse sequences: homonuclear decoupling and dilute spin NMR in solids, *Chem. Phys. Lett.* **155,** 341–346 (1989).